International Journal of Pharmacology

ISSN 1811-7775

science alert

ansinet
Asian Network for Scientific Information

OPEN ACCESS International Journal of Pharmacology

ISSN 1811-7775
DOI: 10.3923/ijp.2024.1281.1291

Research Article
Alendronate Sodium Combined Glatiramer Acetate Nanocomplex Suppresses Pancreatic Cancer Cell Growth

[1] Ashraf Bahi el-din Abdel-Naim and [2]Usama Ahmed Fahmy

[1]Department of Pharmacology and toxicology, Faculty of Pharmacy, King Abdulaziz University, Jeddah, Saudi Arabia
[2]Center of Excellence for Drug Research and Pharmaceutical Industries, King Abdulaziz University, Jeddah, Saudi Arabia

Abstract

Background and Objective: Pancreatic cancer (PC) have increased significantly in recent years. Asymptotic manifestation, which can lead to tumor cells entering the metastatic stage before detection, is one of the main problems with PC. Therefore, the current investigation was conducted to give an effective treatment method, in which pancreatic cancer was suppressed using an optimized alendronate sodium (ALS) and glatiramer acetate (GA) (ALS-GA) nanoconjugate. **Materials and Methods:** To obtain an optimized ALS-GA nanoconjugates, Box-Behnken design was used. Design-Expert® Software Version 12 (Stat-Ease Inc., Minneapolis, Minnesota, United States) software was used while size and zeta potential was selected as responses. To evaluate the anticancer efficacy, analysis of IC_{50}, Bcl-2, Bax, p53, etc., were tested. **Results:** The particle size of the optimized nanoconjugate was found to be 28.4±1.2 nm. The cytotoxicity in terms of IC_{50} for ALS-GA nanoconjugate was found to be (4.13± 0.2 µg/mL) enhanced than GA alone (12.6±0.2 µg/mL) or ALS alone (20.4±0.4 µg/mL). Besides, Bax, Bcl-2, p53 and caspase 3 estimation also showed superior apoptotic activity for ALS-GA nanoconjugate. However, as compared to ALS alone, GA alone, nanoconjugate showed increased expression of TNF-α and anticancer activity. **Conclusion:** These data revealed superiority of ALS-GA nanoconjugate over individual components, making it a novel approach for PC treatment.

Key words: Optimization, formulation, cationic peptides, apoptosis, PANC1cell lines, zeta potential

Citation: Abdel-Naim, A.B. and U.A. Fahmy, 2024. Alendronate sodium combined glatiramer acetate nanocomplex suppresses pancreatic cancer cell growth. Int. J. Pharmacol., 20: 1281-1291.

Corresponding Author: Usama Ahmed Fahmy, Center of Excellence for Drug Research and Pharmaceutical Industries, King Abdulaziz University, Jeddah, Saudi Arabia

Funding: This research work was funded by Institutional Fund Projects under grant No. (IFPIP: 2071-166-1443).

Competing Interest: The authors have declared that no competing interest exists.

Data Availability: All relevant data are within the paper and its supporting information files.

INTRODUCTION

Cancer kills more people worldwide than any other type of tumor. As many as 1.88 million people become sufferers of the disease in 2018. In 2020, pancreatic cancer (PC) will account for 10% of all new cases of cancer and 9.4% of all estimated number of deaths due to cancer, making it the second leading cause of cancer-related mortality recorded behind lung cancer (18%)[1].

Apoptosis and anti-angiogenic effects of bisphosphonates have been proven *in vitro* in numerous cancer cells. As a result, bisphosphonates are being investigated as possible adjutant agents for intestinal cancers[2,3]. Due to their ability to decrease protein prenylation and compromise cellular function and survival, nitrogen-containing bisphosphonates have been reported to offer superior anti-tumor effects *in vivo*[4]. Alendronate sodium (ALS) is a bisphosphonate that may both be employed as a medicinal drug and as a targeted moiety. Osteoporosis, Paget's disease, primary hyperparathyroidism, malignant hypercalcemia and metastatic bone disorders are among the conditions for which ALS is given orally as a therapy option[5,6]. The ALS's cytotoxicity might be put to good use[7,8]. Researchers have shown that ALS can act synergistically to slow tumor growth and migration, making it a potentially useful cytotoxic drug[9,10]. As an alternative to conventional treatments like chemotherapy and radiation, cancer immunotherapies are now available[11]. Innate immune responses are activated by the majority of immunostimulants being studied for cancer immunotherapy. Costimulatory molecules and antigen presentation are increased when immunostimulants are applied in the presence of antigen. This can lead to the production of tumor-specific T-cells[12].

There have been reports that glatiramer acetate (GA), a positively charged polypeptide, can deliver plasmid DNA into cells[13]. The FDA-approved relapsing-remitting multiple sclerosis medication, has recently been demonstrated to remain at the injection site and form aggregates *in situ*, suggesting that it might be useful as a drug delivery agent[14].

The recent introduction and formulation of nanoparticle-based pharmaceutical actives has opened several doors for the diagnosis, treatment and cure of difficult diseases. A variety of nanostructures may be turned into smart systems through fine-tuning their sizes, shapes, surface modification, surface features and materials employed. The controlled release treatment provided by these nanosized structures can be delivered to specific tissues or locations. This extended and targeted medication administration reduces drug toxicity and improves patient compliance with fewer dose intervals[15]. As a result of nanotechnology advancements in cancer treatment, there are several avenues to overcome current obstacles[16]. As a medication delivery system, nanostructures provide several benefits. For cancer therapy and imaging, nanoparticles, tubes, nanovesicles, nanocaps, nanoemulsions, nanodots and nanowires are amongst the nanostructures being extensively researched[17]. It is also worth noting that drug nanocomplexes can be classified as nanocarriers since the drug is attached to or loaded within the nanocarrier. Polymer, lipid, peptide, or even DNA can be used as a carrier molecule[18-20]. As a result, nanoparticles that are well-designed allow for targeted medicine delivery to tumors or certain cell populations without negatively affecting healthy tissues and organs[21].

Ideally, a nanoparticulate-based drug delivery system (DDS) would concentrate in the desired organ or tissue while also penetrating target cells to release the bioactive substance. Nanoparticulate DDS, for instance liposomes and micelles, are often used for the purpose of enhancing the efficacy of drug and DNA delivery and site-specific targeting[22]. Although many drug carriers are currently under development, only a few number of them have been shown to be effective in getting pharmaceuticals and DNA into cells by bypassing the endocytic route, therefore increasing medication efficacy and DNA integration into the cell genome[23,24]. Advances in nanomedicine have led to the formulation of drugs and other physiologically relevant chemicals that are incorporated into nanoscale structures platform for an enhanced targeted delivery to sites of action. Thus, in this work, the effects of nanocomplex of ALS (a nitrogen-containing bisphosphonate) with GA for the management of pancreatic cancer.

MATERIALS AND METHODS

Study area: Formulation was carried out at Nanotechnology Laboratory in 2022, Faculty of Pharmacy, King Abdulaziz University, Jeddah, Saudi Arabia. However, IC_{50}, Bax, Bcl-2, p53 and caspase 3 were carried out by Dr. Essam Rashwan at Cell Culture Lab (VACSERA-Egypt) in 2022.

Chemicals and materials: The ALS was a gift from SPIMACO (Qassim, Saudi Arabia), GA was purchased from Natco Pharma Pharmaceutical company (Banjara Hills, Hyderabad, India), Human Pancreatic carcinoma PANC1 was kindly supplied from cell culture, departments (VACSERA-Egypt).

Methods

Experimental design for optimization of ALS-GA nanoconjugates: To obtain an optimized ALS-GA nanoconjugates, Box-Behnken design was used. The independent variables were ALS concentration

Table 1: Independent variables' levels and the constraint of the dependent variable (particle size constraint) used in the Box-Behnken design for the optimization of ALS-GA nanoconjugates

	Levels		
Independent variable	(-1)	(0)	(+1)
X_1: ALS molar concentration	0.50	1.25	2.00
X_2: Incubation time (min)	5.0	17.5	30.0
X_3: Sonication time (min)	2.0	8.5	15.0
Responses	Desirability constraint		
Y: Particle size (nm)	Minimize		

ALS: Alendronate sodium and GA: Glatiramer acetate

Table 2: Combination of variables' levels along with their resultant particle size for ALS-GA nanoconjugates experimental runs prepared as per Box-Behnken design

	Independent variables			
Experimental run#	ALS molar concentration (mM)	Incubation time (min)	Sonication time (min)	Particle size (nm)
F1	1.25	5.0	2.0	302
F2	1.25	17.5	8.5	275
F3	0.50	30.0	8.5	243
F4	2.00	17.5	2.0	423
F5	2.00	17.5	15.0	421
F6	1.25	30.0	2.0	356
F7	2.00	5.0	8.5	398
F8	1.25	30.0	15.0	347
F9	2.00	30.0	8.5	453
F10	1.25	17.5	8.5	276
F11	0.50	5.0	8.5	166
F12	1.25	17.5	8.5	275
F13	1.25	5.0	15.0	266
F14	0.50	17.5	2.0	220
F15	0.50	17.5	15.0	183

ALS: Alendronate sodium and GA: Glatiramer acetate

(ALS conc., mM, X_1), incubation time (IT, min, X_2), in addition to sonication time (ST, min, X_3), while the studied response was particle size (PS, nm, Y). The independent variables employed in this study along with their levels were depicted in Table 1. The 15 experimental runs that were generated by Design-Expert® Software Version 12 (Stat-Ease Inc., Minneapolis, Minnesota, United States) by combining various levels of the independent variables as well as their measured particle size are shown in Table 2. On the basis of Analysis of Variance (ANOVA) provision, the significance of the variables' effects and the interactions between them on the measured size was determined. A $p<0.05$ indicates a statistical significance. With respect to coded factors, the equation that represents the best fitting sequential model for size was computed. The selection of the best fitting model was according to the highest determination coefficient (R^2) as well as the least predicted residual sum of squares (PRESS). For selection of the optimized formulation, numerical optimization technique was applied. The objective outcome was to minimize particle size to its least possible value.

Particle size measurement: Using the Nano-ZS analyzer, the ALS-GA particle size was determined using the dynamic light scattering technique (Malvern Instrument, Worcestershire, UK). Samples were appropriately diluted using the formulation's aqueous phase to reach an optimal count of 50-200 kilocounts per second (kcps). The data are the average of five measurement±standard deviation (SD).

Characterization of the optimized ALS-GA: For analysis of the optimized ALS-GA, a transmission electron microscope (JEOL GEM-1010, JEOL Ltd., Akishima, Tokyo, Japan) was employed by The Regional Center for Mycology and Biotechnology (Al- Azhar University, Cairo, Egypt). A single drop of the diluted GA dispersion was put to a carbon-coated grid, adsorbed on the carbon film for three minutes. Then, the adsorbed GA was stained using phosphotungstic acid (1% w/v, pH 6.8). Following the removal of the extra stain, the grid was carefully air-dried. The coated samples were then examined at 30,000 times magnification and micrographs were recorded. Further, three freeze-thaw testing cycles (between -20 and 25°C) were conducted in order to investigate the stability of the optimized ALS-GA. Samples were then analysed for particle size and compared to those of freshly prepared GA.

Cytotoxicity study of optimized ALS-GA via MTT assay: The PANC1 cells (5×10^3 cells/well -96 well plate) were seeded. After 24 hrs adherence, the optimized ALS-GA conjugate was

added at appropriate concentrations prior to incubation for 24 hrs. Then, growth medium was replaced with 200 µL of PBS and 20 µL MTT stock solution (5 mg/mL in PBS) and incubated for 4 hrs. Subsequently, MTT solution was replaced with DMSO for 30 min. Measurement of absorbance of formazan crystals was performed at 570 nm using microplate reader. Cell viability was expressed as percentage of absorbance related to untreated cells.

Caspase 3 estimation: The caspase 3 level was determined using a colorimetric assay kit (BioVision, Milpitas, CA, USA) in treated PANC1 cells with varied substances. The PANC1 cells (3×10^6 cells/well) were cultivated for this purpose and treated with a variety of substances, including normal saline, ALS alone, GA and ALS-GA. Additionally, treated cells were suspended in lysate buffer (ice-cold) and incubated on ice for ten minutes. After 10 min, cells were centrifuged at 10,000 g for 1 min and the acquired samples were utilized for caspase-3 estimate as per the manufacturer's instructions and the evolved colour at 405 nm was evaluated using a microplate reader[25].

Real-Time Polymerase Chain Reaction (RT-PCR) for estimation of Bcl-2, Bax, p53, caspase 3 and TNF-α: The RT-PCR was used to evaluate Bcl-2, Bax, p53, caspase 3 and TNF-α expression. The PANC1 cells were cultured with ALS-raw, GA and ALS-GA for the indicated times. The cell fraction was used to extract RNA and then cDNA was synthesized. Using the Gene Runner software, primers for Bcl-2, Bax, p53, caspase 3 and TNF-α were designed. The produced samples were quantified in triplicate for expression and the samples were normalized using actin[26,27].

Statistical analysis: All experimental values were expressed as Mean±SD. One Way ANOVA followed by *post-hoc* analysis using Tukey's multiple comparison test was used where $p<0.05$ was considered to be statistically significant.

RESULTS

Experimental design for optimization of ALS-GA nanoconjugates

Fit statistics and diagnostic analysis: The quadratic model, as demonstrated by its highest R^2 and least PRESS, was the best fitting model amongst the investigated sequential models for the particle size of the generated ALS-GA nanoconjugates; the model fit analysis findings were shown in Table 3.

Amongst the explored sequential models, the greatest correlation (R^2) and least predicted residual sum of square (PRESS); was found to be those corresponding to the quadratic model; accordingly it was considered as the best fitting model for the ALS-GA conjugates particle size; results of the model fit analysis were summarised in Table 3. Further, adequate precision value indicated was 310.82, suggesting an adequate signal-to-noise ratio and, as a result, the model was a suitable tool to explore the experimental 'design space'. Figure 1 illustrated the diagnostic plots for the observed response (particle size) generated, as another statistical parameter to assess the goodness of fit for the selected sequential model.

Figure 1(a), displaying normal probability plots of residuals, shows a linear trend indicating the normal distribution of residuals, with no transformation being required for the data. Figure 1(b-c), which present the externally studentized residuals versus either predicted response or run number, respectively, show randomly spread points that lie within the boundaries, indicating the absence of continuous error or lurking variable that may interfere with the observed size. In addition, the predicted particle size values vs actual values' plot, shown in Fig. 1d, implies that the predicted and actual particle sizes are in a reasonable agreement, confirming that the model is valid.

Variables' effect on particle size (Y): It is well established that the average size of nanoscaled drug delivery systems is a key factor impacting the penetration of active therapeutics through biological membranes. Table 2 showed that the developed ALS-GA nanoconjugates ranged from 166 to 423 nm. According to results from ANOVA, the computed F-value of 9669.31 ($p<0.0001$) confirmed the validity of the proposed quadratic model, with as little as 0.01% chance that this high value could be attributed to noise. In terms of coded factors, the equation for the quadratic model was created as follows:

$$Y = 275.33+110.37\ X_1+33.37\ X_2-10.50\ X_3-5.50\ X_1X_2+8.75\ X_1X_3+6.75\ X_2X_3+16.83\ X_1^2+22.83\ X_2^2+19.58\ X_3^2$$

Analysis of variance revealed that all the independent variables exhibited a highly significant effect on the size as depicted by a p-value of less than 0.0001 for all the linear (X_1, X_2 and X_3) and quadratic (X_1^2, X_2^2 and X^2) terms. In addition, all the interaction terms were also significant (95% level of significance). Figure 2(a-d) displayed perturbation plot and contour (Two-Dimensional, 2D) plots for the investigated variables' effects on the size as well as their interaction.

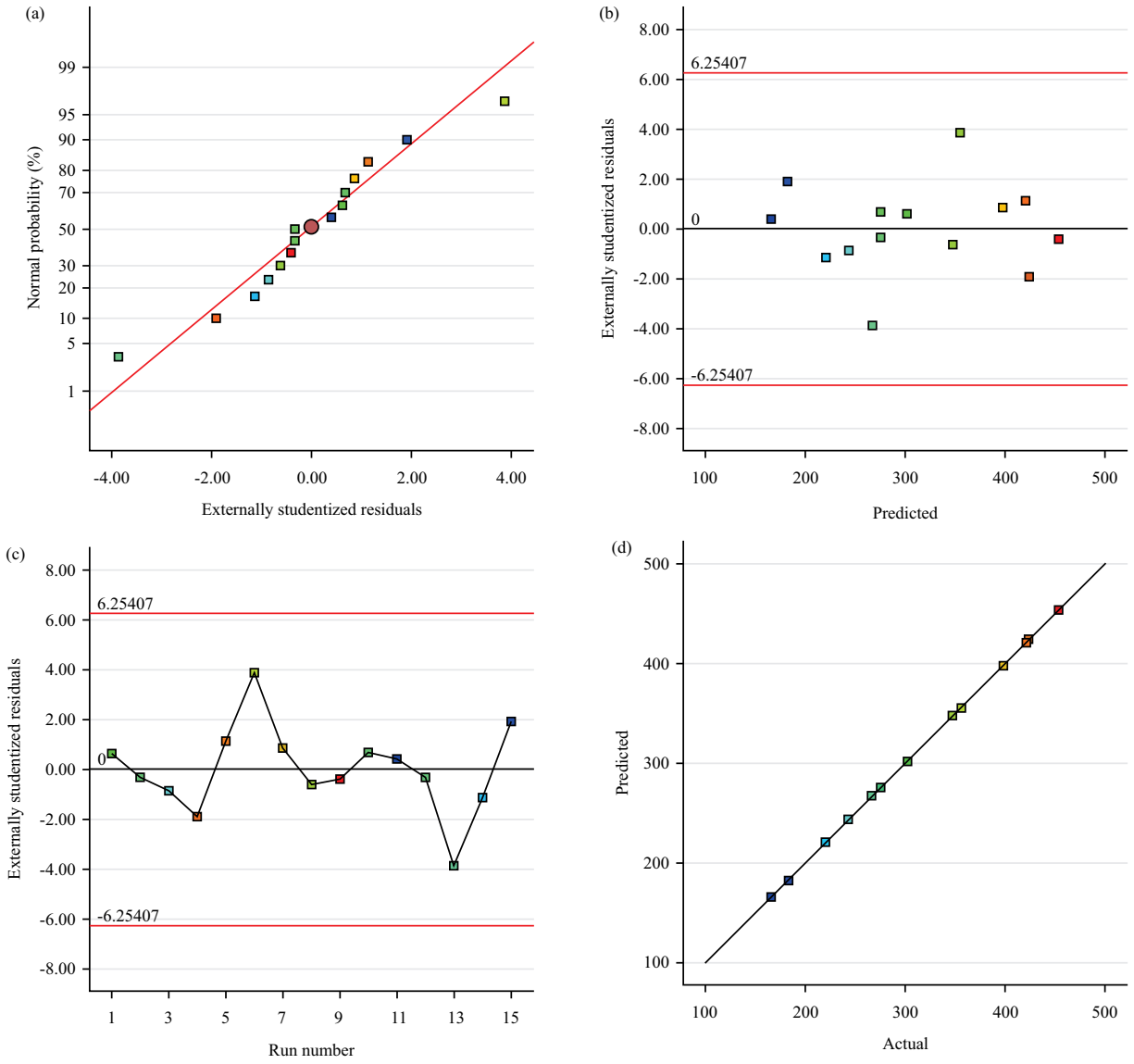

Fig. 1(a-d): Particle size diagnostic plots of ALS-GA nanoconjugates, (a) Residuals' normal probability plot, (b) Externally studentized residuals vs. predicted size, (c) Externally studentized residuals vs. run number and (d) Predicted vs. actual size plot

Figure 2(a-d) show that particle size is directly proportional to both ALS molar conc. and IT, while it is inversely proportional to the ST. The positive sign of both X_1 and X_2 coefficients and the negative sign of X_3 confirms these findings. The order of the effects of variables on particle size, determined by the value of the corresponding coefficients in the sequential model equation, was found to be ALS molar conc. >IT>ST. Previous data have reported that at higher drug levels particle size of nanoconjugates increase. A proper explanation for the observed particle size increase when incubation duration is concomitantly increased, could be associated with increasing liability of drug conjugation with GA. Clearly, at longer incubation time, the quantity of drug molecules binding to GA increases, leading to an increase in the average particle size of the conjugates. Furthermore, the negative influence of sonication time on particle size has been documented earlier for a variety of nanoparticulate systems. It could be due to the cavitation forces created by the sonicator's ultrasonic waves. Such forces could perhaps lead to a diminished particle size as fractionation of the developed conjugates could possibly occur.

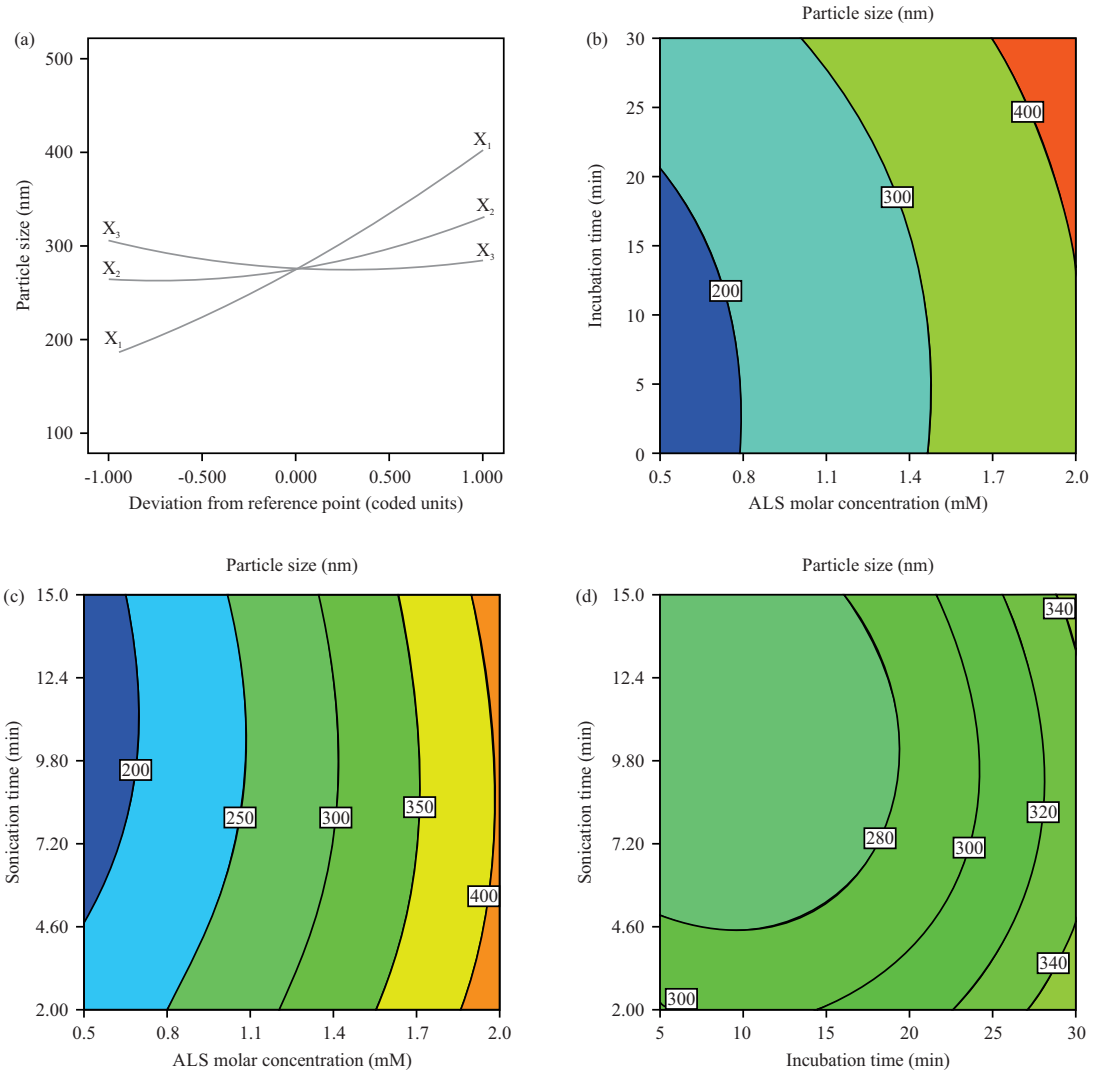

Fig. 2(a-d): Perturbation plot, (a) Contour 2D-plots and (b-d) Influence of ALS concentration (X_1), incubation time (X_2) and sonication (X_3) on the particle size of ALS-GA conjugates

Optimization: The optimal levels of the tested independent variables, which could achieve the previously set goal of obtaining the least possible particle size upon combination, were predicted as follows: 0.518 mM for ALS molar conc., 5.4 min for ST and 14.2 min for IT. The optimized ALS-GA nanoconjugate was formulated, thereafter testing for particle size as well as the biological activity in cancer cells was carried out. The optimization approach validity is demonstrated by the low percentage error of 1.25% between the expected (160 nm) and measured particle size (158 nm).

ALS-GA nanoconjugates cytotoxic activity in PANC1: The optimized formula of ALS-GA nanoconjugate was assessed for cytotoxicity in PANC1 cancer cell line along with free ALS and free GA. The ALS-GA nanoconjugate (IC_{50} value of 4.30±0.190) is significantly more toxic than GA (12.60±0.58 µg/mL) in PANC1pancreatic cells. The optimized formulation of the nanoconjugate is three fold more effective than corresponding free GA. On the other hand when comparing free ALS with others, free ALS appears to be less toxic than both GA and ALS-GA nanoconjugate in PANC1 cells as represented in Fig. 3.

ALS-GA nanoconjugates modulate Bax and Bcl-2 protein levels: A probable explanation to the Bax expression is associated with pro-apoptotic events, whereas the Bcl-2 expression could be due to antiapoptotic activities.

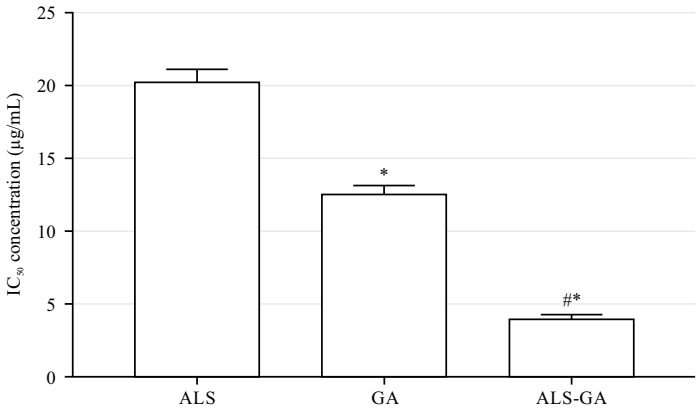

Fig. 3: IC_{50} of the ALS, GA and ALS-GA in the PANC1 cells

Values of the four independent experiments are Mean±SD, *Significant vs ALS, p<0.05 and #Significant vs GA

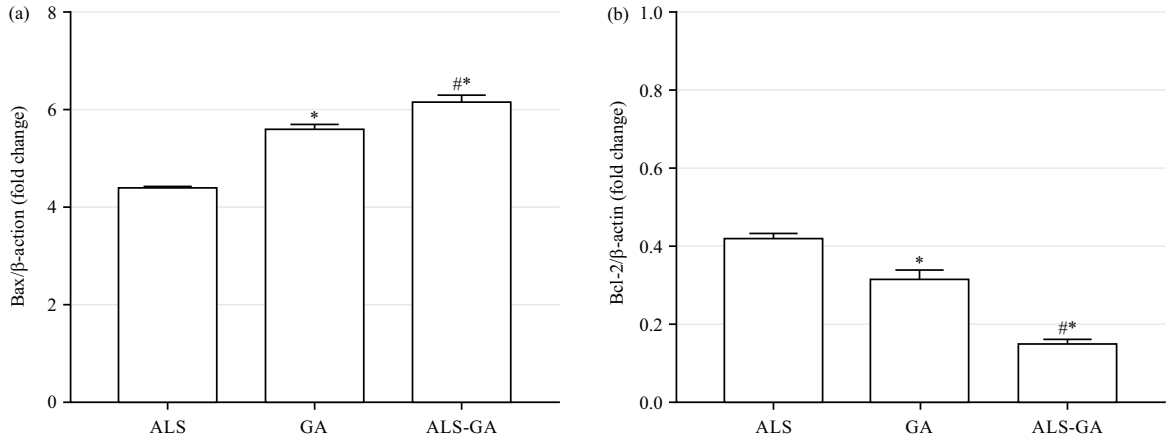

Fig. 4(a-b): Modulation of ALS, GA and ALS-GA treatments on (a) Bax and (b) Bcl-2 protein concentrations in PANC1 cells

Values of the four independent experiments are Mean±SD, *p<0.05 for significance vs control (p<0.05) and #Significance vs control

Table 3: Model fit statistics for the particle size of ALS-GA nanoconjugates

Source	Sequential p-value	Lack of fit p-value	SD	R^2	Adjusted R^2	Predicted R^2	PRESS
Linear	<0.0001	0.0007	20.07	0.9603	0.9495	0.9417	6515.72
2FI	0.7404	0.0005	21.86	0.9658	0.9401	0.9298	7842.96
Quadratic	<0.0001	0.1517	1.13	0.9999	0.9998	0.9992	93.50

Figure 4a illustrates the modulation of Bax levels in PANC1 cells upon exposure to various experimental conditions. Interestingly, all the treatments, including ALS, seemed to enhance significantly (p<0.001) Bax levels when compared to untreated cells. A significant marked enhancement of the Bax expression was observed upon GA treatment, in comparison to ALS (p<0.001). It was notably observed that the most prominent effect was for PANC1 cells treated with ALS-GA nanoconjugates for 24 hrs.

The complete opposite pattern for Bcl-2 levels, compared to the corresponding Bax protein trend was detected (Fig. 4b). Taking these different expression pattern into consideration, we can conclude that ALS-GA nanoconjugate induce apoptosis in PANC1 cell line.

Indeed, apoptosis is regarded as a decisive parameter for quantifying the activity of anticancers. Indeed, apoptosis is regarded as a decisive parameter for quantifying the activity of anticancers. Thus, the drug's anticancer potency is determined by a balance of pro and anti-apoptotic proteins. In the current work, administering ALS-GA nanoconjugate dramatically raised the expression of pro-apoptotic proteins such as Bax, caspase 3 and p53 while

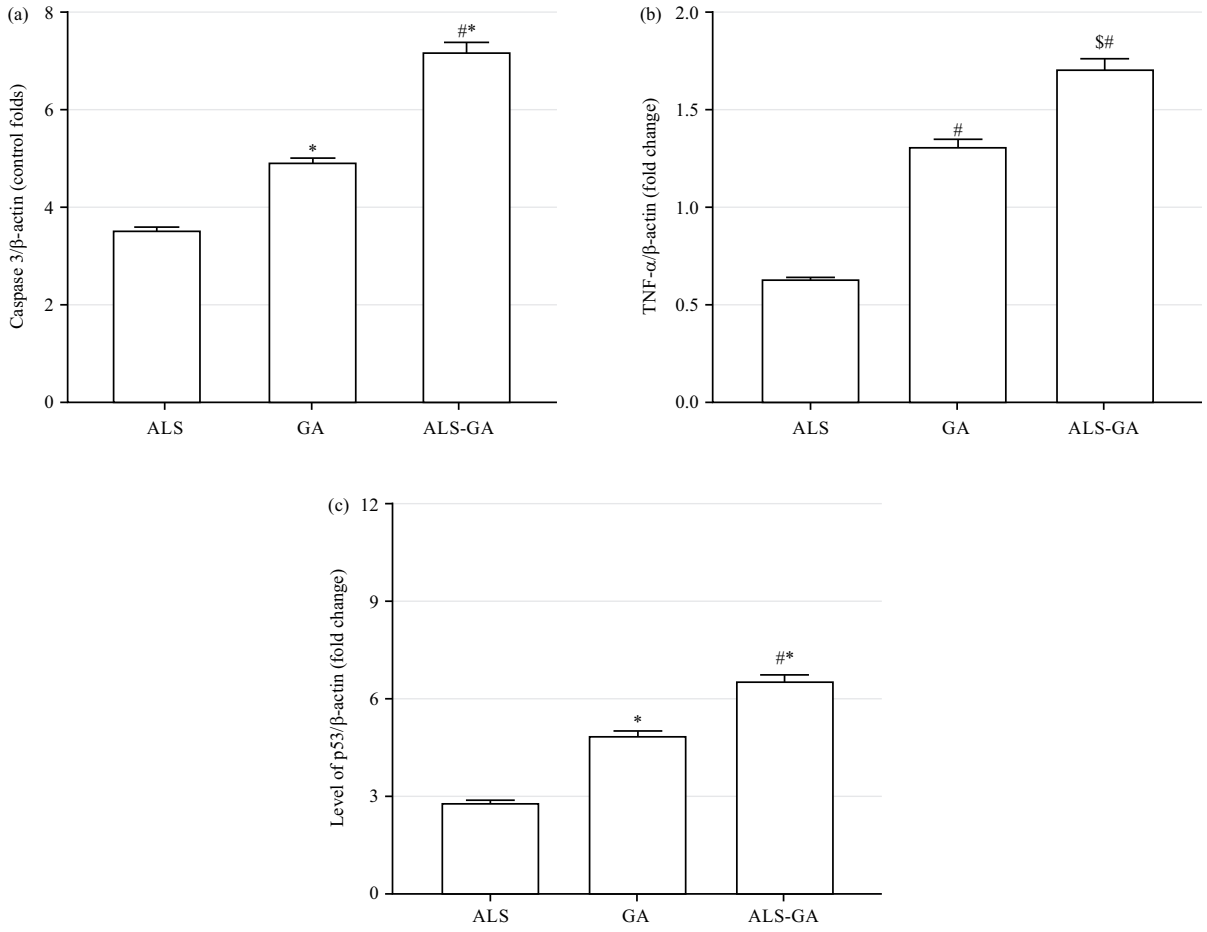

Fig. 5(a-c): Expression level of different pro and anti-apoptotic proteins such as (a) Caspase 3, (b) TNF-α and (c) p53 against PANC1 cells when treated with ALS, GA alone and ALS-GA nanoconjugate

*p<0.05 for significance vs. ALS and #p<0.05 for significance vs GA

decreasing the expression of anti-apoptotic protein Bcl-2 compared to ALS and GA alone (Fig. 5a-c). However, as compared to ALS alone, GA demonstrated enhanced apoptotic activity.

DISCUSSION

Both the incidence and frequency of PC has increased dramatically in recent years[28,29]. Therefore, an ALS and GA nanoconjugate was produced, developed and described in the current research. The formulation's anticancer potential was confirmed in PANC1 cells by the use of MTT assay, a variety of apoptotic measures, gene expression analysis, inflammatory markers and cell cycle arrest research. Implementing the experimental design along with optimization procedure aimed to explore the effect of the selected factors on the observed response and to optimize the variables' levels for the purpose of achieving objectives that have been previously established[30,31]. The efficacy of nano-scaled particulate delivery systems entering the body is highly dictated by the size of the particles delivered. Collectively, current findings indicated that there is a proportional increase in the size of the spheres, as the GA molar ratio and incubation duration are increased. It is possible that the cationic character of GA is responsible for its impact. After obtaining the optimized formula, *in vitro* experiments were conducted, where the GA ability to augment the antineoplastic activity of a subtoxic concentration of ALS against PANC1 cells was tested[32,33]. It is recognized that PANC1 cells serve as an-established experimental model for investigating the toxic potential of ALS alone or combined with other anticancer drugs on PANC1. In fact, we imply an improved therapeutic potential of ALS-GA after obtaining data of the different IC_{50} values (Fig. 3), under our experimental conditions.

A substantial difference was noted between the IC_{50} values recorded for either ALS alone or GA. Undoubtedly, because of the synergistic cytotoxic effect achieved by conjugating ALS to the peptide GA (ALS-GA nanoconjugates), carrying out this research is imperative from several perspectives. Regardless of the global widespread use of ALS for conventional therapies as well as non-conventional therapie (e.g., treatment of cancer), clinically significant adverse effects have been reported earlier, even when the drug is administered at therapeutic doses. Additional evidence of the improved anticancer activity of ALS-GA nanoconjugates was obtained when assessing the impact on the cell cycle phases of PANC1 tumor cells. These findings were in close agreement with previously published data, which has demonstrated the ALS capability to trigger apoptosis in a variety of cell types, including vascular endothelial cells. Immune T cells and mast cells. Noteworthy, the pro-apoptotic action of ALS occurs at minimal (sub-toxic) concentrations and is attributable to the synergism obtained when the drug is combined with GA, in the contrary to the proven relative minimum activity of the drug in its free form (ALS). The capacity of this synergistic combination to modify Bax (raise) (Fig. 5a) and Bcl-2 (reduce) (Fig. 5b) protein levels in PANC1 cells added further support to the findings on ALS-GA pro-apoptotic activity. As previously reported by Zhan *et al.*[7], the potential of ALS to trigger cell death via the elevated activation of pro-apoptotic components, for instance caspase-3 and Bax, while concurrently decreasing Bcl-2, was consistent with the current findings of the present study. Despite the fact that the ALS-GA combination demonstrated the substantially greatest antineoplastic activity, the activity of GA alone is equally noteworthy. According to the results of nearly all of the *in vitro* cell experiments, the anticancer activity of GA used solely at IC_{10} concentration was found to be greater than that of the drug in its free form (ALS). It should be pointed out that this is consistent with multiple recent studies of Huang *et al.*[28] and Lasoń *et al.*[29], wherein it was revealed that GA was able of suppressing the epidermal growth factor receptors (EGFR) 1 and 2. The current findings further demonstrated that combining this natural substance along with another antineoplastic therapeutics resulted in providing markedly potent anticancer activity than either treatment alone.

Conventional DDSs are unable to deliver antineoplastic therapeutics in the optimum and greatest effective concentration necessary to trigger tumor cell death and as a result, crippling side effects are experienced. Nanoconjugates containing the combination of two antineoplastic drugs provide a unique approach to increase the estimated therapeutic index and pharmacokinetic behaviour of chemotherapeutic drugs. Based on the evaluation of the physicochemical properties of the formulated ALS-GA nanoconjugates; namely particle size, surface characteristics and stability profile, it is strongly believed that intraperitoneal administration of these nanoconjugates could follow the five steps of the CAPIR cascade in a highly efficient manner. In order to explore the pharmacokinetic profile of ALS-GA nanoconjugates in animal models, more *in vivo* investigations will be necessary in the future.

CONCLUSION

Using Box-Behnken-based design, multiple formulae were created an optimal ALS-GA nanoconjugate with the smallest particle size. The therapeutic effectiveness of the optimized ALS-GA nanoconjugate, ALS alone and GA alone was determined by treating PANC1 cells. To assess anti-PC effects, cells were treated with the optimized formula to evaluate the cytotoxicity, Bax, Bcl-2, p53, caspase 3 and TNF-α. Results showed super anti-PC activity. Overall, based on these results for ALS-GA nanoconjugate, it is possible to conclude that it might be a unique and promising PC treatment way and *in vivo* studies required to confirm these results.

SIGNIFICANCE STATEMENT

This work aims to explore the efficacy of the novel electrostatic complex against pancreatic cancer cells, different formulae with different molar ratios of alendronate and glatiramer acetate were created. Nitrogen-containing bisphosphonates have been shown to have better anti-tumor effects *in vivo* because of their capacity to reduce protein prenylation and jeopardize cellular viability and function. One bisphosphonate that can be used as a medication and a targeted moiety is alendronate sodium (ALS). Positively charged polypeptide glatiramer acetate (GA) has been reported to carry plasmid DNA into cells. This study revealed superiority of ALS-GA nanoconjugate as a prospective formula against pancreatic cancer cells. *In vivo* studies should be follow this work to evaluate its effectiveness in humans.

ACKNOWLEDGMENT

The authors gratefully acknowledge the technical and financial support provided by the Ministry of Education and King Abdulaziz University, DSR, Jeddah, Saudi Arabia.

REFERENCES

1. Xi, Y. and P. Xu, 2021. Global colorectal cancer burden in 2020 and projections to 2040. Transl. Oncol., Vol. 14. 10.1016/j.tranon.2021.101174.
2. de Rosa, G., G. Misso, G. Salzano and M. Caraglia, 2013. Bisphosphonates and cancer: What opportunities from nanotechnology? J. Drug Delivery, Vol. 2013. 10.1155/2013/637976.
3. Ang, C., E. Doyle and A. Branch, 2016. Bisphosphonates as potential adjuvants for patients with cancers of the digestive system. World J. Gastroenterol., 22: 906-916.
4. Green, J.R., 2003. Antitumor effects of bisphosphonates. Cancer, 97: 840-847.
5. Sultana, S., R. Ali, S. Talegaonkar, F.J. Ahmad, G. Mittal and A. Bhatnagar, 2013. *In vivo* lung deposition and sub-acute inhalation toxicity studies of nano-sized alendronate sodium as an antidote for inhaled toxic substances in sprague dawley rats. Environ. Toxicol. Pharmacol., 36: 636-647.
6. Dolatabadi, J.E.N., H. Hamishehkar, M. de la Guardia and H. Valizadeh, 2014. A fast and simple spectrofluorometric method for the determination of alendronate sodium in pharmaceuticals. Bioimpacts, 4: 39-42.
7. Zhan, X., L. Jia, Y. Niu, H. Qi and X. Chen *et al*., 2014. Targeted depletion of tumour-associated macrophages by an alendronate-glucomannan conjugate for cancer immunotherapy. Biomaterials, 35: 10046-10057.
8. Moreira, M.S., E. Katayama, A.C. Bombana and M.M. Marques, 2005. Cytotoxicity analysis of alendronate on cultured endothelial cells and subcutaneous tissue. A pilot study. Dent. Traumatol., 21: 329-335.
9. Gschwantler-Kaulich, D., S. Weingartshofer, T.W. Grunt, M. Mairhofer, Y. Tan, J. Gamper and C.F. Singer, 2017. Estradiol impairs the antiproliferative and proapoptotic effect of zoledronic acid in hormone sensitive breast cancer cells *in vitro*. PLoS ONE, Vol. 12. 10.1371/journal.pone.0185566.
10. Rouach, V., I. Goldshtein, I. Wolf, R. Catane and G. Chodick *et al*., 2018. Exposure to alendronate is associated with a lower risk of bone metastases in osteoporotic women with early breast cancer. J. Bone Oncol., 12: 91-95.
11. Bonaventura, P., T. Shekarian, V. Alcazer, J. Valladeau-Guilemond and S. Valsesia-Wittmann *et al*., 2019. Cold tumors: A therapeutic challenge for immunotherapy. Front. Immunol., Vol. 10. 10.3389/fimmu.2019.00168.
12. Temizoz, B., E. Kuroda and K.J. Ishii, 2016. Vaccine adjuvants as potential cancer immunotherapeutics. Int. Immunol., 28: 329-338.
13. Alhakamy, N.A. and C.J. Berkland, 2019. Glatiramer acetate (copaxone) is a promising gene delivery vector. Mol. Pharm., 16: 1596-1605.
14. Song, J.Y., N.R. Larson, S. Thati, I. Torres-Vazquez and N. Martinez-Rivera *et al*., 2019. Glatiramer acetate persists at the injection site and draining lymph nodes *via* electrostatically-induced aggregation. J. Controlled Release, 293: 36-47.
15. Khan, A.U., M. Khan, M.H. Cho and M.M. Khan, 2020. Selected nanotechnologies and nanostructures for drug delivery, nanomedicine and cure. Bioprocess Biosyst. Eng., 43: 1339-1357.
16. Misra, R., S. Acharya and S.K. Sahoo, 2010. Cancer nanotechnology: Application of nanotechnology in cancer therapy. Drug Discovery Today, 15: 842-850.
17. Chaturvedi, V.K., A. Singh, V.K. Singh and M.P. Singh, 2019. Cancer nanotechnology: A new revolution for cancer diagnosis and therapy. Curr. Drug Metab., 20: 416-429.
18. Ajithkumar, K.C. and K. Pramod, 2018. Doxorubicin-DNA adduct entrenched and motif tethered artificial virus encased in pH-responsive polypeptide complex for targeted cancer therapy. Mater. Sci. Eng.: C, 89: 387-400.
19. Irby, D., C. Du and F. Li, 2017. Lipid-drug conjugate for enhancing drug delivery. Mol. Pharm., 14: 1325-1338.
20. Abioye, A.O., G.T. Chi, A.T. Kola-Mustapha, K. Ruparelia, K. Beresford and R. Arroo, 2016. Polymer-drug nanoconjugate-An innovative nanomedicine: Challenges and recent advancements in rational formulation design for effective delivery of poorly soluble drugs. Pharm. Nanotechnol., 4: 38-79.
21. Shen, B., Y. Ma, S. Yu and C. Ji, 2016. Smart multifunctional magnetic nanoparticle-based drug delivery system for cancer thermo-chemotherapy and intracellular imaging. ACS Appl. Mater. Interfaces, 8: 24502-24508.
22. Trochilin, V.P., 2005. Recent advances with liposomes as pharmaceutical carriers. Nat. Rev. Drug Discovery, 4: 145-160.
23. Maheshwari, A., R.I. Mahato, J. McGregor, S.O. Han, W.E. Samlowski, J.S. Park and S.W. Kim, 2000. Soluble biodegradable polymer-based cytokine gene delivery for cancer treatment. Mol. Ther., 2: 121-130.
24. Delcassian, D. and A.K. Patel, 2020. Nanotechnology and Drug Delivery. In: Bioengineering Innovative Solutions for Cancer, Ladame, S. and J.Y.H. Chang (Eds.), Academic Press, Cambridge, Massachusetts, ISBN: 9780128138861, pp: 197-219.
25. Alhakamy, N.A., O.A.A. Ahmed, U.A. Fahmy and S. Md, 2021. Apamin-conjugated alendronate sodium nanocomplex for management of pancreatic cancer. Pharmaceuticals, Vol. 14. 10.3390/ph14080729.
26. Naguib, M.J., S. Salah, S.A. Abdel Halim and S.M. Badr-Eldin, 2020. Investigating the potential of utilizing glycerosomes as a novel vesicular platform for enhancing intranasal delivery of lacidipine. Int. J. Pharm., Vol. 582. 10.1016/j.ijpharm.2020.119302.

27. Sharma, N., P. Madan and S. Lin, 2016. Effect of process and formulation variables on the preparation of parenteral paclitaxel-loaded biodegradable polymeric nanoparticles: A co-surfactant study. Asian J. Pharm. Sci., 11: 404-416.
28. Huang, W., C.P. Tsui, C.Y. Tang and L. Gu, 2018. Effects of compositional tailoring on drug delivery behaviours of silica xerogel/polymer core-shell composite nanoparticles. Sci. Rep., Vol. 8. 10.1038/s41598-018-31070-9.
29. Lasoń, E., E. Sikora and J. Ogonowski, 2013. Influence of process parameters on properties of nanostructured lipid carriers (NLC) formulation. Acta Biochim. Pol., 60: 773-777.
30. Ghaderi, S., S. Ghanbarzadeh, Z. Mohammadhassani and H. Hamishehkar, 2014. Formulation of gammaoryzanol-loaded nanoparticles for potential application in fortifying food products. Adv. Pharm. Bull., 4: 549-554.
31. El-Helw, A.R.M. and U.A. Fahmy, 2015. Improvement of fluvastatin bioavailability by loading on nanostructured lipid carriers. Int. J. Nanomed., 10: 5797-5804.
32. Khalaf, N., H.B. El-Serag, H.R. Abrams and A.P. Thrift, 2021. Burden of pancreatic cancer: From epidemiology to practice. Clin. Gastroenterol. Hepatol., 19: 876-884.
33. McGuigan, A., P. Kelly, R.C. Turkington, C. Jones, H.G. Coleman and R.S. McCain, 2018. Pancreatic cancer: A review of clinical diagnosis, epidemiology, treatment and outcomes. World J. Gastroenterol., 24: 4846-4861.